

## Observation of Ionospheric Cavities

A. Y. Wong, T. Tanikawa, and A. Kuthi

*Department of Physics, University of California, Los Angeles, Los Angeles, California 90024*

(Received 11 September 1986)

The observation of the change in the ionospheric density profile and the creation of a density cavity at the critical height by high-power radio waves is made by the time-of-flight radar scattering technique. Small-scale cavities imbedded inside a large cavity are inferred from the suppression of the photoelectron-enhanced plasma lines near the critical height.

PACS numbers: 94.20.-y, 52.35.Mw, 52.40.Db

We wish to report the direct measurement of the ionospheric cavity created near the critical layer where the local plasma frequency matches the frequency of the high-power, incident electromagnetic (em) wave. Cavities are density cavities created by either the ponderomotive force of the incident em wave (em cavities),<sup>1</sup> or the enhanced electrostatic (es) waves (es cavities),<sup>2</sup> or the thermal pressure of heated plasma particles (thermal cavities).<sup>3</sup> These various cavities can be distinguished by the time scale of development and the size of the perturbations. The size of em cavities is typically tens of meters, while that of es cavities is of the order of tens of centimeters; thermal cavities are of the order of a kilometer. Both em and es cavities evolve in an ion time scale which can be shorter than the electron-ion collision time, while thermal cavities must evolve in the thermalization time scale which is much longer than the collision time and can be of the order of seconds depending upon the altitude of interest. These cavities are important in the interpretation of a number of experimental observations in the ionosphere. The direct conversion of em waves into es waves requires the presence of small-scale density inhomogeneities such as es cavities.<sup>4</sup> The long decay-time constant of the electron plasma waves (EPW's) after the termination of the heating wave can be explained in terms of their being trapped inside cavities.<sup>2,5</sup> The strong interaction between two EPW's enhanced at normally very separate locations according to the undisturbed density profile can be explained by the generation of cavities with steep local density gradients.<sup>2,6</sup> The direct observation of cavities therefore provides a coherent explanation of a number of nonlinear processes in the active modification of the ionosphere by high-power em waves. The ability to produce cavities also leads to a method of remote excitation of low-frequency ion acoustic waves in the ionosphere. The excitation of ion acoustic waves at frequencies much greater than the collision frequency is a manifestation of the action by the ponderomotive force associated with the incident em wave and/or the enhanced es waves.

A series of experiments were conducted at the Arecibo Observatory during August 1984, March 1985, and February 1986. An hf wave at 5.1 MHz was sent upward in the O-mode polarization with the maximum

power of 400 kW and an antenna gain of  $\sim 23$  dB in a pulsed mode. This condition corresponds to a wave electric field strength of up to  $\sim 0.35$  V/m in the ionosphere at a 200-km altitude without taking into account the swelling of the field due to the plasma collective effect. The swelling effect can enhance the wave electric field to  $\sim 2.7$  V/m near the reflection layer<sup>7</sup> at the incident power of 400 kW. This value well exceeds the threshold field strength of  $\sim 0.7$  V/m for the parametric decay instability.<sup>8</sup> The EPW's of 35-cm wavelength were detected as upper and lower sidebands of the Thomson-backscattering return of a 2-MW radar at 430 MHz. The density profile was measured by our monitoring the time of arrival of this return which yields the height information<sup>9</sup>; the shifted frequency of the return yields the plasma frequency at that height.<sup>10</sup> In our experiment, a short Thomson-radar pulse of 20  $\mu$ s was sent to the ionosphere and the radar receiver with a 50-kHz bandwidth was tuned to receive the sideband frequency of 430 MHz +  $f_{pl}$ , where  $f_{pl}$  is the frequency of the EPW whose wavelength is 35 cm. The data-acquisition system was set to acquire data with the sampling period of 4  $\mu$ s. The height resolution for this system was approximately 1 km from use of the observed overall density-gradient scale length [ $L \equiv n_0 (dn/dh)^{-1}$ , where  $n_0$  is the local plasma density and  $h$  is the altitude] of 40 km as deduced from the Thomson scattering from the background electrons. The heater pulse at 5.1 MHz had an on period of 25 ms and an off period of the same duration [Fig. 1(a)]. By sampling the Thomson return after the heater pulse was turned on [the 430-MHz radar pulses designated as "in" in Fig. 1(a)], we measured the density perturbation produced by the heater. The difference between the arrival times of the Thomson-radar return shifted by the frequency of the EPW at various levels of the heater power reflects the change in the density profile as a function of the heater power [see Fig. 1(b)]. A delayed arrival implies that the scattering point has moved higher or the initial density is now at a greater height. Since the uhf radar signal does not undergo significant refraction, this is an accurate method of our determining the location of plasma waves and hence the plasma densities at various altitudes.<sup>11</sup>

Using the above experimental procedure, we measured

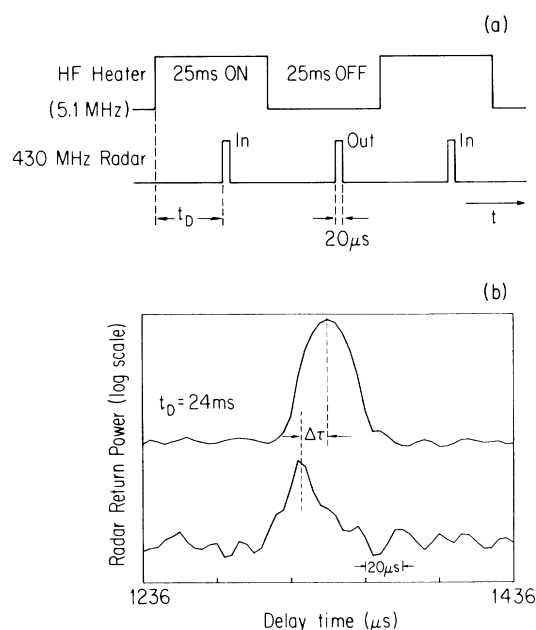


FIG. 1. Experimental procedure. (a) Pulse sequence showing the hf heater pulse and the 430-MHz diagnostic Thomson-radar pulse. (b) Thomson-radar returns at 435.1 MHz due to scattering by the electron plasma waves at 5.1 MHz for two different levels of the heater power, 100 kW (the lower curve) and 400 kW (the upper curve). The difference in the arrival times,  $\Delta\tau$ , reflects the change in the density profile. The data were taken at 16:40 AST on 28 February 1986.

the density profiles at three different levels of the heater power as shown in Fig. 2. In each case, the pulse sequence in Fig. 1(a) was used and 1000 shots were accumulated for each point. It took approximately 1 min to acquire each datum point. The background density profile (indicated by the crosses in Fig. 2) was measured just before the hf transmitters were turned on to begin the three runs at different hf-power levels. It was measured by EPW's excited by photoelectrons.<sup>9</sup> In order to confirm that the density-profile modification described below is an hf-induced phenomenon, we repeated this experimental sequence at least ten times (over a five-day period) during each of the three Arecibo experimental campaigns in 1984, 1985, and 1986. All runs yielded results similar to those shown in Fig. 2. When the duty cycle of the hf heater is 50% in a period of 50 ms, it takes 200 kW of the heater power to modify the density profile from an unperturbed profile of  $L \approx 40$  km to a steeper one ( $L \approx 32$  km) with a gentler profile ( $L \approx 200$  km) just below it. The pulsing scheme that we have chosen allows sufficient energy deposition to the heating region over many hf pulses; at the same time, each off period is long enough for the hf-enhanced EPW's to decay<sup>2</sup> so that the photoelectron-enhanced plasma lines can be studied during the hf off periods by use of the radar "out" pulses in Fig. 1(a), as discussed later. At the heater power of 400

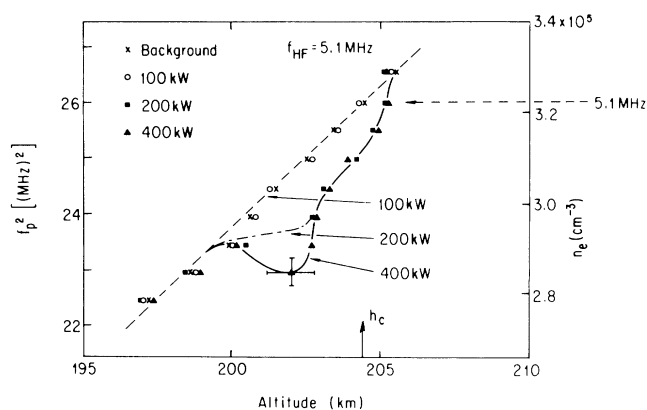


FIG. 2. Density profiles as calculated from the time-of-flight measurements of the Thomson radar at three different levels of the heater power. Altitude of a given density ( $n \propto f_p^2$ ) is determined from the time of flight of the backscattered radar pulse whose frequency is centered at  $430 \text{ MHz} + f_{pl}$  as determined by the setting of the radar receiver, where  $f_{pl}$  is the frequency of the plasma wave which scatters the radar. The local plasma frequency,  $f_p(h) = \omega_p(h)/2\pi$ , at a given altitude  $h$  is determined from the dispersion relation  $\omega_{pl}^2 = \omega_p^2(h) + 3k^2 \delta v_c^2 + \omega_c^2 \sin^2 \theta$ . The critical height  $h_c$  is determined from  $\omega_0 = \omega_p(h_c)$ , where  $\omega_0$  is the angular frequency of the incident hf wave. The data were taken between 15:29 and 16:15 AST on 28 February 1986.

kW, a density cavity is formed near the critical height where the plasma frequency equals the incident hf frequency. The depth of the cavity is observed to be  $\sim 7\%$ . All the observations were made under steady-state pulsing conditions which allow thermal and particle equilibrium to be established. The recent numerical study<sup>3</sup> of heat-transport processes in the F-region ionosphere has shown that it takes approximately 90 s for the thermal pressure during heating to create a large-scale density cavity near the reflection layer for the 5.1-MHz heater. Starting from a "cold turnon" (i.e., the hf transmitters were off for at least an hour before they were turned on), we first established the background condition and then observed the density-profile modification. The density profile was significantly changed only when the heater power exceeded 200 kW (or the vacuum wave-field strength of  $\sim 0.25$  V/m at 200-km altitude).

Since the amplitude of the swelled field of the incident em wave for the power of 400 kW near the reflection layer exceeds the threshold field strength for the parametric decay instability by a factor of  $\sim 4$ , large-amplitude EPW's are expected to exist in the large density cavity shown in Fig. 2. The ponderomotive force associated with these large-amplitude EPW's can dig small-scale (order of  $10\lambda_D - 100\lambda_D$  or 10 cm  $\sim$  100 cm) density cavities inside the large density cavity.<sup>5</sup>

Although the Thomson diagnostic radar has a height resolution of  $\sim 1$  km, a novel method has been used to infer the existence of small-scale es cavitons imbedded

inside the large density cavity shown in Fig. 2. This method utilizes the fact that EPW's of long wavelengths can couple with density perturbations of shorter wavelengths to form nonresonant modes which are strongly Landau damped.<sup>12</sup> This coupling, which has been experimentally observed in the laboratory,<sup>13</sup> gives an additional damping mechanism to the EPW's enhanced by the photoelectron flux. This effective damping can be included in the following estimate for the received intensity of photoelectron-enhanced plasma lines<sup>9,14</sup>:

$$P_R(f_{pl})/P_T \propto n_f L / h^2 \gamma_{\text{eff}}. \quad (1)$$

Here,  $P_R(f_{pl})/P_T$  is the ratio of the backscattered radar power received at  $430 \text{ MHz} + f_{pl}$  to the transmitted power,  $h$  is the altitude of the EPW's which backscatter the radar,  $L$  is the density gradient scale length at  $h$ ,  $n_f$  is the density of photoelectrons of velocity  $v = 2\pi f_{pl}/k_0$  which are responsible for the excitation of the EPW's of  $f_{pl}$  and  $k_0$ , and  $\gamma_{\text{eff}}$  is the effective damping rate of the photoelectron-enhanced EPW's. Therefore, the intensity of photoelectron-enhanced plasma lines is inversely proportional to the effective damping rate  $\gamma_{\text{eff}}$ . The increase in  $\gamma_{\text{eff}}$  due to the nonresonant mode coupling,  $\Delta\gamma_{\text{eff}}$ , is given by<sup>12,13</sup>

$$\Delta\gamma_{\text{eff}} \sim |\delta n/n_0| \omega_{pl}(h), \quad (2)$$

where  $\delta n$  is the amplitude of the density perturbations and  $n_0$  is the background plasma density.

We have used the above concept in our interpretation of the effect of hf heating on photoelectron-enhanced plasma lines from the bottom side of the daytime ionosphere. Photoelectron-enhanced plasma lines were detected during the hf off periods by means of the radar pulses designated as "out" in Fig. 1(a). Each out pulse was placed just before the turnon of the next hf pulse. By that time, the EPW's excited by the hf wave had completely decayed,<sup>2</sup> making it possible to detect the radar returns due solely to the photoelectron-enhanced EPW's. As shown in Fig. 3, the intensities of the photoelectron-enhanced plasma lines from the bottom side and the top side of the ionosphere are compared with each other. Since the photoelectron-enhanced plasma lines from the top side of the ionosphere come from the region well beyond the hf cutoff point, they are not affected by the incident hf wave and are used as reference signals [see Fig. 3(a)]. As can be seen in Figs. 3(b) and 3(c), the photoelectron-enhanced plasma line at 5.1 MHz from the bottom-side ionosphere has been found to be sensitively dependent on the power of the incident em wave; its intensity is reduced by a factor of  $\sim 3.5$  when the heater power is increased from 100 to 400 kW. This suppression of photoelectron-enhanced plasma lines was observed only in close proximity to the critical height ( $5.05 \text{ MHz} \leq f_{pl} \leq 5.15 \text{ MHz}$ ). According to Eq. (1), the received radar power of photoelectron-enhanced plasma lines is proportional to the local density-gradient

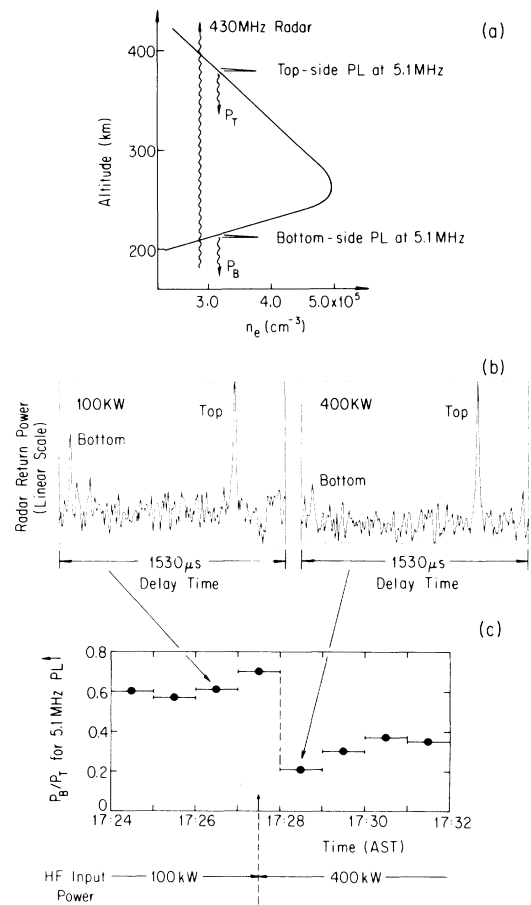


FIG. 3. Suppression of photoelectron-enhanced plasma line in the bottom side of the ionosphere under the existence of small-scale es cavitons. (a) Schematic of the locations of the bottom-side and top-side plasma lines at 5.1 MHz. (b) Radar returns from the bottom and top locations at two different levels of hf power, 100 and 400 kW. The heater-induced density perturbations at 400 kW cause the reduction in the intensity of the bottom-side plasma line. (c) Dependence of  $P_B/P_T$ , the ratio of the intensity of the bottom-side photoelectron-enhanced plasma line to that of the top-side one, on the heater power. The measurements were performed during the off period of the heater, i.e., the radar out pulses shown in Fig. 1(a) were used for the measurements. The data were taken between 17:24 and 17:32 AST on 28 February 1986.

scale length  $L$ . However, the gentle change (the reduction in  $L$  is roughly 20% of the initial value) in the overall density profile around the critical height ( $\sim 204 \text{ km}$ ) as depicted in Fig. 2 cannot account for the preferential suppression of photoelectron-enhanced plasma lines. Using Eq. (2), we find that a small-scale ( $\sim 10\lambda_D$ ) density perturbation of  $|\delta n/n_0| \approx 1\%$  near the critical height can explain the observed preferential suppression of photoelectron-enhanced plasma lines.<sup>13</sup>

In conclusion, our experiment has revealed a picture of

the formation of cavitons under high-power em irradiation of the ionosphere. The ponderomotive force associated with intense EPW's creates small-scale density cavities inside a large-scale density cavity which is a result of the electron heating and the particle and thermal transport. The main heating takes place in the vicinity of the critical layer where the intensity of oscillating fields is large. Recent data from both the low-latitude (at the Arecibo Observatory in Puerto Rico) experiment using the chirped 430-MHz radar diagnostic<sup>15</sup> and the high-latitude [at the High Power Auroral Simulation Observatory (HIPAS) in Alaska] experiment using the pulsed hf wave diagnostic<sup>16</sup> have also revealed similar perturbations of the density profile near the critical height under high-power em irradiation.

We wish to acknowledge the useful discussions with Dr. M. Shoucri at the University of California, Los Angeles and the assistance from the staff of the Arecibo Observatory, especially from Dr. M. Sulzer, Dr. H. M. Ierkec, and Mr. D. Albino. The Arecibo Observatory is part of the National Astronomy and Ionospheric Center, which is operated by Cornell University under contract with the National Science Foundation. This research was supported by the Institute of Geophysics and Planetary Physics at the Los Alamos National Laboratory and the Department of Physics at the University of California, Los Angeles.

<sup>1</sup>J. A. Fejer, H. M. Ierkec, R. F. Woodman, J. Röttger, M. Sulzer, R. A. Behnke, and A. Veldhuis, *J. Geophys. Res.* **88**, 2083 (1983).

<sup>2</sup>A. Y. Wong, J. Santoru, C. Darrow, L. Wang, and J. G. Roederer, *Radio Sci.* **18**, 815 (1983).

<sup>3</sup>M. M. Shoucri, G. J. Morales, and J. E. Maggs, *J. Geophys. Res.* **89**, 2907 (1984).

<sup>4</sup>A. Y. Wong, G. J. Morales, D. Eggleston, J. Santoru, and R. Behnke, *Phys. Rev. Lett.* **47**, 1340 (1981); G. J. Morales, A. Y. Wong, J. Santoru, L. Wang, and L. M. Duncan, *Radio Sci.* **17**, 1313 (1982).

<sup>5</sup>T. Tanikawa, A. Y. Wong, and D. L. Eggleston, *Phys. Fluids* **27**, 1416 (1984).

<sup>6</sup>T. Tanikawa, A. Y. Wong, T. Crowley, and A. Kuthi, *Bull. Am. Phys. Soc.* **30**, 1465 (1985).

<sup>7</sup>R. B. White and F. F. Chen, *Plasma Phys.* **16**, 565 (1974). The measured density gradient scale length of  $\sim 40$  km and the em wave frequency of 5.1 MHz are used to estimate the swelled field strength.

<sup>8</sup>A. Y. Wong and R. J. Taylor, *Phys. Rev. Lett.* **27**, 644 (1971); D. F. DuBois and M. V. Goldman, *Phys. Rev.* **164**, 207 (1967).

<sup>9</sup>K. O. Yngvesson and F. W. Perkins, *J. Geophys. Res.* **73**, 97 (1968).

<sup>10</sup>The plasma frequency at a given height  $h$ ,  $\omega_p(h)$ , is given by  $\omega_p^2(h) = \omega_{pi}^2 - 3k\delta v_e^2 - \omega_c^2 \sin^2\theta$ , where  $\omega_{pi}$  is the frequency of the electron plasma wave detected by the Thomson radar,  $k_0$  is the wave number of the wave ( $2\pi/35$  cm<sup>-1</sup> for our case),  $v_e$  is the electron thermal velocity,  $\omega_c$  is the electron cyclotron frequency, and  $\theta$  is the angle between the geomagnetic field and the wave-propagation direction.

<sup>11</sup>The change in electron temperature  $T_e$  causes a much smaller change in the arrival time of the radar return than the change in plasma density does since  $3k\delta v_e^2 \ll \omega_p^2$  for EPW's of 35-cm wavelength.

<sup>12</sup>W. L. Kruer, *Phys. Fluids* **15**, 2423 (1972).

<sup>13</sup>B. H. Quon, A. Y. Wong, and B. H. Ripin, *Phys. Rev. Lett.* **32**, 406 (1974).

<sup>14</sup>F. Perkins and E. E. Salpeter, *Phys. Rev.* **139**, A55 (1965).

<sup>15</sup>W. Birkmayer, T. Hagfors, and W. Kofman, *Phys. Rev. Lett.* **57**, 1008 (1986).

<sup>16</sup>A. Y. Wong, P. J. Barrett, P. Y. Cheung, K. Lam, and J. Stanley, University of California, Los Angeles, Plasma Physics Group Report No. 994, June 1986 (to be published).